







Article

Picoplankton Distribution and Activity in the Deep Waters of the Southern Adriatic Sea

Danijela Šantić ^{1,*} , Vedrana Kovačević ², Manuel Bensi ², Michele Giani ² ,
Ana Vrdoljak Tomaš ¹ , Marin Ordulj ³ , Chiara Santinelli ², Stefanija Šestanović ¹,
Mladen Šolić ¹  and Branka Grbec ¹ 

¹ Institute of Oceanography and Fisheries, Šetalište Ivana Meštrovića 63, POB 500, 21000 Split, Croatia

² National Institute of Oceanography and Applied Geophysics, Borgo Grotta Gigante 42/c, 34010 Sgonico (Ts), Italy

³ University of Split, University Department of Marine Studies, Ruđera Boškovića 37, 21000 Split, Croatia

* Correspondence: segvic@izor.hr; Tel.: +385-21-408-006; Fax: +385-21-358-650

Received: 19 July 2019; Accepted: 8 August 2019; Published: 10 August 2019



Abstract: Southern Adriatic (Eastern Mediterranean Sea) is a region strongly dominated by large-scale oceanographic processes and local open-ocean dense water formation. In this study, picoplankton biomass, distribution, and activity were examined during two oceanographic cruises and analyzed in relation to environmental parameters and hydrographic conditions comparing pre and post-winter phases (December 2015, April 2016). Picoplankton density with the domination of autotrophic biomasses was higher in the pre-winter phase when significant amounts of picoautotrophs were also found in the meso- and bathy-pelagic layers, while *Synechococcus* dominated the picoautotrophic group. Higher values of bacterial production and domination of High Nucleic Acid content bacteria (HNA bacteria) were found in deep waters, especially during the post-winter phase, suggesting that bacteria can have an active role in the deep-sea environment. Aerobic anoxygenic phototrophic bacteria accounted for a small proportion of total heterotrophic bacteria but contributed up to 4% of bacterial carbon content. Changes in the picoplankton community were mainly driven by nutrient availability, heterotrophic nanoflagellates abundance, and water mass movements and mixing. Our results suggest that autotrophic and heterotrophic members of the picoplankton community are an important carbon source in the food web in the deep-sea, as well as in the epipelagic layer. Besides, viral lysis may affect the activity of the picoplankton community and enrich the water column with dissolved organic carbon.

Keywords: picoplankton community; deep-sea; Southern Adriatic; Mediterranean Sea

1. Introduction

Autotrophic members of the picoplankton community are important primary producers, while bacteria are consumers of the dissolved organic matter that can originate from primary production, thus transferring carbon towards higher trophic levels. Bacteria represent the main component of plankton, which is involved in the degradation of organic matter and in transforming inorganic compounds into the shapes adequate for primary producers. The role of the picoplankton community has become more important in oligotrophic and phosphorus-limited (P-limited) areas, such as the open sea area of the Adriatic Sea (Mediterranean Sea), where bacteria, *Synechococcus*, *Prochlorococcus*, and picoeukaryotes play an important role in the production and flow of biomass and energy [1–3] than in eutrophic areas. However, previous studies on picoplankton communities were mostly focused on investigating the epipelagic layer (i.e., depths less than 200 m). The deep-sea is characterized by the absence of light, i.e., conditions that are unfavorable for the primary production. Tanaka and

Rassoulzadegan [4] pointed out the importance of bacteria and their biomass in carbon flux in the deep-sea. Moreover, Arístegui et al. [5] have highlighted that the deep ocean represents a key site for remineralization of organic matter and long-term carbon storage. The discovery of cyanobacteria *Synechococcus* in the deep part of the Adriatic Sea revealed that they could be used to gain a better understanding of the effects of deep-ocean convection, such as ventilation and renewal of deep waters [6]. Hence, the vertical distribution of the picoplankton in the open southern Adriatic Sea, below the euphotic zone, has recently started to be investigated more intensively [7–10]. Aerobic anoxygenic phototrophs (AAPs), a bacterial group recently discovered in the Adriatic Sea [11,12] and primarily unknown in the investigated area, are up to $3 \times$ bigger than other bacterial cells [13,14], and hence they could represent a remarkable source of carbon in the marine environment. These photoheterotrophic microorganisms can harvest light energy using pigment bacteriochlorophyll *a* to supplement their primarily organotrophic metabolism only in the presence of oxygen [15].

The Adriatic Sea is an elongated semi-enclosed basin of the Eastern Mediterranean Sea. According to its morphology and bathymetry, it can be divided into three sub-basins (northern, middle, and southern). The Southern Adriatic Pit (hereafter SAP) is the deepest area, with a depth reaching ~1250 m. Adriatic is characterized by a cyclonic basin-scale circulation. Through the Strait of Otranto at its southern end (~80 km wide, with a sill depth of ~800 m) [16,17], the Adriatic exchanges water and mass with the adjacent Ionian Sea. The Eastern Adriatic Current (EAC) brings northward warm and saline waters from the Ionian Sea and the Western Adriatic Current (WAC), transporting southward colder and fresher waters [18]. Waters from the Ionian Sea enrich the P-limited Adriatic Sea [19,20] with nutrients and organic substances, causing changes in the food web [21] and the distribution of organisms [6,8,10,22]. The prevalent heat and salt import from the Ionian involve the surface and intermediate layers of the Adriatic Sea, between the surface and 800 m depth. According to Gačić et al. [23], periodical changes in the sense of the rotation between cyclonic and anticyclonic phases of the North Ionian Gyre (NIG) deviate the branch of the Atlantic water, entering the Eastern Mediterranean through the Strait of Sicily, towards the Adriatic (during anticyclonic phase) or towards the Cretan and Levantine basins (during cyclonic phase). Under these two opposite conditions, changes in the heat and salt content of the SAP may occur out of phase compared to those observed in the Levantine basin [24]. Moreover, water masses flowing into the Adriatic along its eastern flank have important ecological implications. Indeed, the pool of available nutrients in the SAP changes according to the phases of the NIG [25–27]. The deep part of the SAP occasionally receives the North Adriatic Dense Water (NAdDW), that ventilates the deepest layers after winter cooling [28,29]. Locally, the open-sea winter convection triggers vertical mixing and produces dense water (Adriatic Deep Water, AdDW) that reaches depths between 300 and 1000 m [30–32]. Subsequently, AdDW outflows across the Strait of Otranto sinks into the Ionian Sea abyss and ventilates the deep layers of the eastern Mediterranean [33].

The picoplankton community is exposed to sudden physical-chemical changes in a dynamic environment. The ability of certain members to acclimate physiologically determine their presence and activity or absence in the water column. Hence, environmental conditions (vertical convection, lateral exchanges, long-term trends, and multiannual oscillatory signals) make the Southern Adriatic an ideal laboratory to study vertical distribution and activity of picoplankton members in the deep zones (below epipelagic layer), where they can represent a significant source of carbon through their biomass.

The primary goal of the ESAW (evolution and spreading of the Southern Adriatic Waters) cruise was to assess and compare the pre-and post-winter hydrographic and environmental (physical, biogeochemical) conditions in the middle and southern Adriatic basins. The objective of the present study was to evaluate for the first time, the abundance of aerobic anoxygenic phototrophs (AAPs) in the deep waters of the Southern Adriatic Pit (hereafter SAP). Beside the AAPs, we determined the distribution of *Synechococcus*, *Prochlorococcus*, picoeukaryotes, and heterotrophic bacteria and estimated their contribution to carbon budget from epipelagic to deep waters. Our study shows and

discusses results obtained from the analysis of picoplankton biomasses and their activity concerning environmental parameters and hydrographic conditions and the effect of grazing and viral lysis.

2. Material and Methods

2.1. Physical and Biochemical Sampling

In this study, we used data collected during the two ESAW cruises (Evolution and spreading of the Southern Adriatic Waters), supported by the EUROFLEETS2 program. The first one was conducted in December 2015 (10–15 December). The second one was conducted in April 2016 (5–10 April), when the hydrographic and environmental conditions were supposed to be changed after the wintertime occurrence of vertical convection, and consequent dense water formation. The intention was to measure the signals of a possible spread of dense water from the middle to the southern Adriatic, because the former may be both an accumulation site and an occasional formation site for dense waters [34]. Here, we focused only on data collected in the SAP, at hydrological stations regularly spaced along a transect between Bari (Ba; Italy) and Dubrovnik (Du; Croatia, Figure 1). A conductivity-temperature-depth (CTD) SBE 911plus probe (Sea-Bird Electronics, Bellevue, WA, USA) measured vertical profiles of temperature (T), conductivity (C), dissolved oxygen (DO), fluorescence, and turbidity. The sampling rate was set to 24 Hz. The T-C sensors were controlled and calibrated before and after the cruise at the Calibration facility center at OGS (Trieste, Italy). For water sampling purposes, the CTD probe was coupled with a rosette sampler, holding 12 Niskin bottles (8-L capacity). Salinity (S), potential temperature (θ), and potential density anomaly (σ_θ) were calculated using the MATLAB toolbox TEOS-10 (<http://www.teos-10.org/software.htm>) and Ocean Data View software [35]. The reference pressure for θ and σ_θ was 0 dbar. Data were processed and quality checked according to MyOcean in situ quality control standards and methodology. The final vertical profiles consisted of the data averaged every 1 dbar, with overall accuracies ± 0.005 °C for T, and ± 0.005 for S, and 2% of DO saturation. Due to the malfunctioning of the SBE43 sensor for DO detection, these data were missing at stations 8 and 9 during the April cruise. The missing profiles were substituted by the data from the closest stations, namely, 7 and 10 (Figure 1), assuming that the main pattern of the vertical structure was similar in the deep SAP region (as compared in Figure 2). Sampling depths for the nutrients and dissolved organic compounds were 2, 45 (56 m in April), 84 (100 m in April), 220 (204 m in April), 400, 500, 662 (600 m in April), 800, 940 (900 m in April), 1000, 1100, 1140 m at station 8; 2, 50 (62 m in April), 96 (100 m in April), 193 (201 m in April), 400 (350 m in April), 520 (missing in April), 700, 800, 900, 1000, 1100, 1208 m at station 9. Dissolved organic carbon (DOC) samples were occasionally sampled at a smaller rate. During sampling, there were no pieces of evidence on neither water leakage from the Niskin bottles nor some other possible source of contamination of the water samples. Moreover, there were no striking patterns among measured parameters which could have indicated such kind of a problem. Therefore, we are confident that the samples were taken correctly.

Water samples for measuring dissolved inorganic nutrient concentrations (nitrite, NO_2 , nitrate, NO_3 , ammonium, NH_4 , phosphate, PO_4 , and silicic acid, H_4SiO_4) were prefiltered through glass-fiber filters (Whatman GF/F) immediately after sampling and stored at -20 °C in polyethylene vials until performing analysis in the on-shore laboratory. The samples were defrosted and analyzed colorimetrically with a QuAAtro Seal Analytical continuous segmented flow analyzer, according to Hansen and Koroleff [36]. Detection limits for the procedure were 0.003 μM , 0.01 μM , 0.04 μM , 0.02 μM , and 0.02 μM for NO_2 , NO_3 , NH_4 , PO_4 , and H_4SiO_4 , respectively. The accuracy and precision of the analytical procedures at low concentrations were checked periodically through the quality assurance program QUASIMEME, and the relative coefficient of variation for five replicates was less than 5%. Internal quality control samples were used during each analysis. As in the case of inorganic nutrients, samples for dissolved organic nitrogen and phosphorus analysis were filtered through Whatman GF/F glass fiber filters, collected in acid-washed polyethylene vials rinsed with seawater, and frozen immediately (-20 °C) until laboratory analysis. Total dissolved inorganic nitrogen

(TDN) and phosphorus (TDP) were determined after quantitative conversion to inorganic N and P by persulfate oxidation [36] and subsequent analyses of nitrate + nitrites and phosphates. Dissolved organic nitrogen (DON) and phosphorus (DOP) were computed from the relationship $\text{DON} = \text{TDN} - (\text{N-NH}_4 + \text{N-NO}_2 + \text{N-NO}_3)$ and $\text{DOP} = \text{TDP} - \text{P-PO}_4$. DOC samples were filtered immediately after collection through 0.2 μm membrane filters (Sartorius, Minisart, SM 16534, Goettingen, Germany) and stored at 4 °C in the dark until analysis (within 3 months). DOC samples were analyzed using a Shimadzu TOC-VCSN. Samples were acidified with 2N HCl and sparged for 3 min with CO₂-free pure air, to remove inorganic carbon before high-temperature catalytic oxidation. One hundred microliters of the sample were injected into the furnace after a four-fold syringe washing. From 3 to 5, replicate injections were performed until the analytical precision was within <2% ($\pm 1 \mu\text{M}$). The calibration curve was determined by using four different solutions of potassium phthalate, in the same concentration range as the samples. The reliability of the measurements was checked daily using consensus reference materials (CRM) kindly supplied by Prof. D. A. Hansell, University of Miami. At least two CRM and two low carbon water (LCW) analyses were performed for each analytical day (measured value = nominal value $\pm 0.5 \mu\text{M}$).

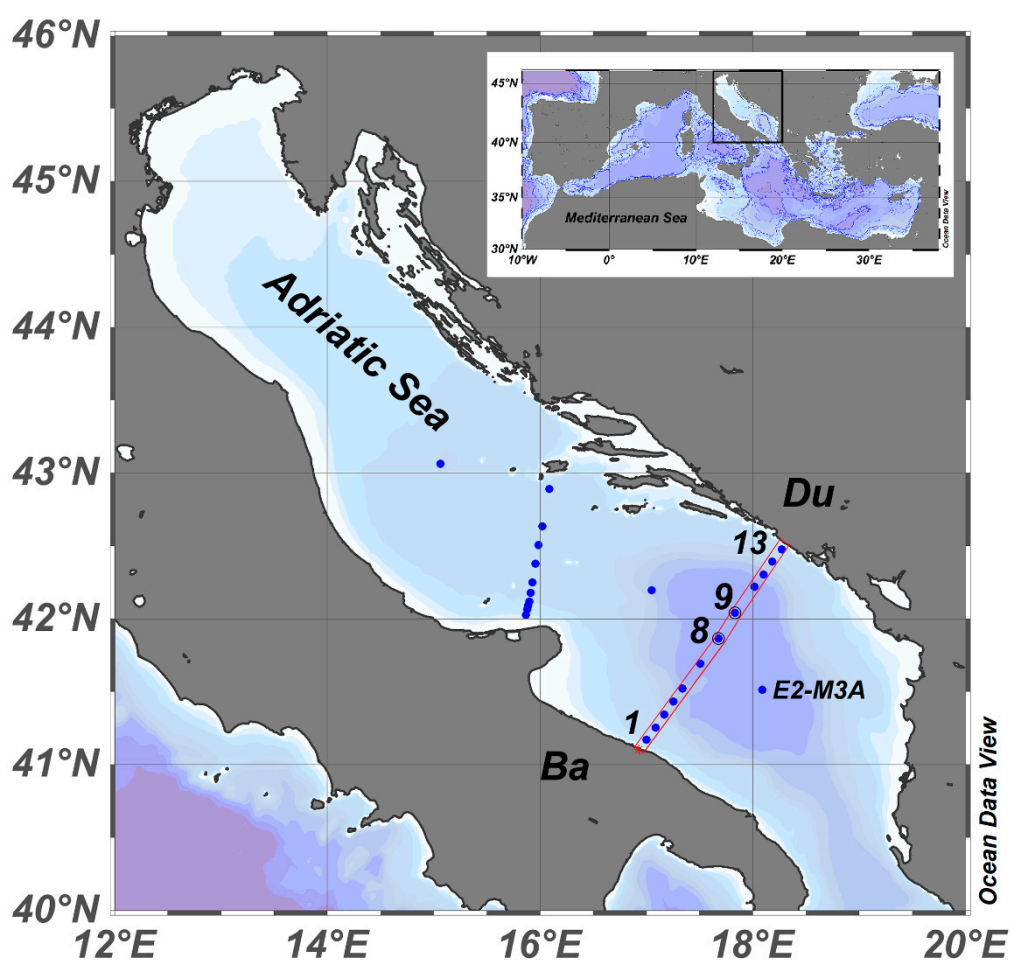


Figure 1. The Adriatic Sea. Blue dots indicate CTD (conductivity-temperature-depth) stations of the ESAW (Evolution and spreading of the Southern Adriatic Waters) cruises. Red line indicates the SAP (Southern Adriatic Pit) transect. Biological sampling concerns stations 8 and 9.

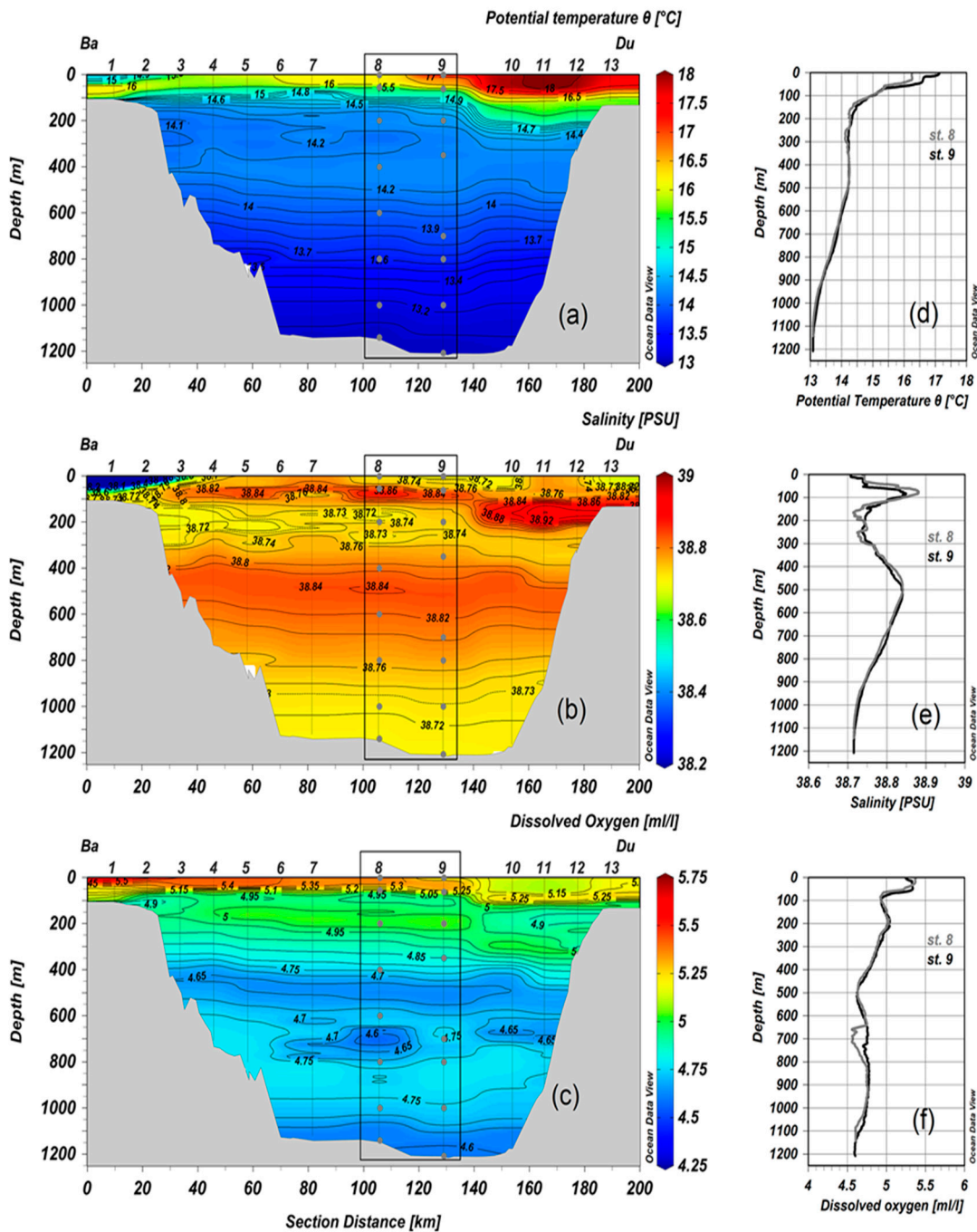


Figure 2. Vertical distribution of (a) potential temperature, (b) salinity, (c) dissolved oxygen, along the Bari-Dubrovnik (Ba-Du) section during the ESAW1 cruise in December 2015. Grey dots indicate locations of picoplankton sampling. Panels (d–f) show the vertical profiles of the same properties at stations 8 and 9.

2.2. Picoplankton Analysis

Sampling depths for the picoplankton analysis were 2, 45 (56 m in April), 220 (204 m in April), 400, 662 (600 m in April), 800, 1000, 1140 m at station 8; 2, 50 (62 in April), 96 (100 m in April), 193 (201 m in April), 400 (350 in April), 520 (missing in April), 700, 800, 1000, 1208 m at station 9. Flow cytometry was used to determine the abundances of *Synechococcus*, *Prochlorococcus*, picoeukaryotes, and heterotrophic bacteria [37]. Samples for autotrophic cells analysis (2 mL) were preserved in 0.5% glutaraldehyde, frozen at $-80\text{ }^{\circ}\text{C}$, and stored until analysis (5–10 days). Samples for analysis of bacteria were preserved

in 2% formaldehyde and frozen until analysis (5–10 days). Autotrophic cells were divided into two groups: cyanobacteria (*Synechococcus* and *Prochlorococcus*) and picoeukaryotes, distinguished according to light scattering, cellular chlorophyll content, and phycoerythrin-rich cells signals, respectively. Bacterial abundance was determined in scatter plots of particle side scatter versus Sybr Green I fluorescence related to cellular nucleic acid content, to discriminate bacteria from other particles. According to the cellular nucleic acid content, the bacterial population is divided into two sub-groups, HNA (High Nucleic Acid content) and LNA (Low Nucleic Acid content) bacteria. Abundances of Sybr Green-I-stained heterotrophic nanoflagellates (HNF) were also determined by cytometry [38]. For obtaining abundances, samples were processed on a Beckman Coulter EPICS XL-MCL with a high flow rate from 1 to 1.2 $\mu\text{L s}^{-1}$. AAPs were sampled only in April and were determined using the protocol described by Mašin et al. [39]. Cells were collected on 0.2- μm polycarbonate (PC) filters by filtration and dyed with 4',6-diamidino-2-phenylindole (DAPI) using 3:1 mixture of Citifluor™ AF1 and Vectashield® after drying. AAP bacteria were enumerated using an Olympus BX51 microscope equipped with an Olympus UPlanSApo 100 \times /1.40 OIL, IR objective, and software for image analysis (CellSens, Münster, Germany). The microscope was equipped with a Hg Lamp U-RFL-T, Olympus, for excitation. Fluorescent images were taken using an XM10-IR camera. Three epifluorescent filter sets were used, DAPI, IR, and chlorophyll, to create the composite image. These images were afterward used for distinguishing between organisms that contain bacteriochlorophyll *a* and chlorophyll *a*, but also for determining the number of heterotrophic bacteria, cyanobacteria, and AAP bacteria in each sample. The abundance of virus-like particles (VLP) was determined, as described in Noble and Fuhrman [40]. Collected samples were preserved in formaldehyde (2%, final concentration), flash-frozen in liquid nitrogen, and stored at $-80\text{ }^{\circ}\text{C}$ until analysis, which was performed in the laboratory immediately after the end of the cruise. Preserved samples (2 mL) were filtered through 0.02- μm pore-size filters (Anodisc; diameter: 25 mm; Al_2O_3 , Whatman, Maidstone, UK) and stained with Sybr Green I (stock solution diluted 1:300). Filters were incubated in the dark for 20 min and mounted on glass slides with a drop of 50% phosphate buffer (6.7 mM, pH 7.8) and 50% glycerol, containing 0.5% ascorbic acid. Slides were stored at a temperature of $-20\text{ }^{\circ}\text{C}$ until analysis. Viral counts were obtained by epifluorescence microscopy (Olympus BX 51, 1250 \times magnification, equipped with a blue excitation filter, Tokyo, Japan) and were expressed as the number of virus-like particles (VLP).

Bacterial cell production was estimated by measuring the incorporation of ^3H -thymidine into bacterial DNA [41]. Methyl- ^3H -thymidine was added to 10 mL samples at a final concentration of 10 nmol (specific activity: 86 Ci mmol^{-1}). Triplicate samples, together with a formaldehyde-killed adsorption control (final concentration: 0.5%), were incubated for one hour. The incubations were stopped with formaldehyde (final concentration: 0.5%). The thymidine samples were extracted with ice-cold trichloroacetic acid (TCA), according to Fuhrman and Azam [41]. Finally, the TCA-insoluble fraction was collected by filtering the samples through 0.2 μm pore size polycarbonate filters.

The biomass of studied picoplankton groups was estimated using the following cell-to-carbon conversion factors: 20 fgC cell^{-1} for heterotrophic bacteria [42,43], 36 fgC cell^{-1} for *Prochlorococcus* [44], 255 fgC cell^{-1} for *Synechococcus* [44], and 2590 fgC cell^{-1} for picoeukaryotes [44] and for AAPs [45].

An empirical model was used to examine the regulation of bacteria by predation [46]. Information about coupling between the abundance of bacteria and heterotrophic nanoflagellates (HNF) would be analyzed using a log-log graph. In particular, this graph included Maximum Attainable Abundance (MAA) and Mean Realized Abundance (MRA) lines. The MAA line described the HNF abundance reached at a given bacterial abundance ($\text{max log HNF} = -2.47 + 1.07 \text{ log bacterial abundance}$). Data close to the MAA line, thus, suggested a strong coupling between the bacteria and HNF abundance, likely interpreted as strong predation on the bacteria [46]. Data positioned below the MRA line instead, suggested that bacterial abundance was not controlled by HNF grazing.

2.3. Statistical Analysis

Pearson's correlation analysis was carried out to examine the relationship between picoplankton community members and environmental variables. The response of the picoplankton community to environmental conditions was analyzed using multivariate statistical analyses. Principal component analysis (PCA) was performed using CANOCO software (<http://www.canoco5.com/>), v5 [47]. PCA is a multivariate statistical method mainly used for data reduction. Analysis attempts were made to identify a few components that explain the major variation within data. In our study, PCA was used to better understand the relationships in multivariate data set between environmental and biological parameters in the SAP. The data were centered and standardized to remove the large differences in abundances between groups. Model results were reproduced in ordination biplots, summarizing the main trends in the data.

3. Results

3.1. Environmental Parameters

The main physical characteristics observed throughout the water column in December 2015 (Figure 2) and April 2016 (Figure 3) were depicted from the distribution of θ , S, and DO concentration along the transect crossing the SAP (roughly from Bari, Italy toward Dubrovnik, Croatia), and from the vertical profiles of the stations 8 and 9, where picoplankton was sampled. Hereafter, we have referred to the upper layer considering the water column between the surface and 100 m depth, to the intermediate layer considering depths between 100 m and 800 m, and to the deep layer considering depths between 800 m and the bottom (~1250 m depth).

In December 2015, the upper layer along the Ba-Du section was quite heterogeneous, which might be due to the contrasting water masses transported into the SAP by the EAC along its eastern side [18], and by the WAC along its western side (Figure 2). In particular, relatively warm and saline waters moving along the eastern margin of the SAP protruded offshore, reaching the central zone of the pit (Figure 2a,b) due to local cyclonic circulation. There, complex features, such as mesoscale eddies, determine large thermohaline differences among close stations, especially between stations 8 and 9. DO distribution (Figure 2c) in the upper layer showed a marked horizontal gradient, with values diminishing from west to east. The upper intermediate layer, between 100 and 400 m, although more homogeneous, was characterized by the presence of water with properties ($\theta > 14.30$ °C and S up to 38.95) typical of the Ionian surface water and the LIWs/CIWs (Levantine/Cretan Intermediate Waters). In the central zone of the SAP, θ gradually decreased with increasing depth, while S had a structure with alternating fresher and saltier layers. Moreover, between 200 and 300 m depth, a branch of fresher water with local S minimum ~38.70 extended from the western flank towards the center of the pit (Figure 2b). In the lower intermediate layer, between 400 and 800 m, instead, S increased up to 38.84, while θ slightly decreased down to 13.60 °C. Overall, layers characterized by high S values were also characterized by reduced DO values (Figure 2c). Notably, two relative oxygen minima were found around 100 m and 500 m depth, in correspondence of relative S maxima (Figure 2e,f). However, there were some differences between stations 8 and 9, concerning mostly S and DO. At station 8 between 100 and 300 m, S values were lower than at station 9 in the same layer. The origin of that fresher layer might be attributable to a detachment of the western-coast vein of freshwater originating from the northern/middle Adriatic, as hinted from the S transect. At station 8, there was a DO minimum at 700 m depth, which was not so evident at the nearby station 9. This seems to be connected with the small scale recirculation of the "old" intermediate layers, associated with the LIW/CIW. The deep layer (>800 m) of the SAP was occupied by relatively cold, less saline, and dense waters likely formed during previous winters in the northern Adriatic. These waters would have been trapped in the deepest part of the SAP, which lies below the depth of the Otranto sill [32,34]. Dense waters coming from the northern Adriatic usually sink to the deep part of the SAP following bathymetric constraints over the slope [48] and they reach their equilibrium depths according to their densities. At the time of the cruise

(December 2015), θ and S in the deep layer had values of 13.10 °C and 38.71, respectively (Figure 2d,e). As far as the oxygen content is concerned, higher values were found between 800 m and 1000 m depth (Figure 2f), and lower values were found below 1000 m depth. This was a sign of water stagnation and lack of ventilation of the deepest part of the SAP during winters before the oceanographic survey, while, likely, relatively dense waters founded their equilibrium depths between 800 and 1000 m.

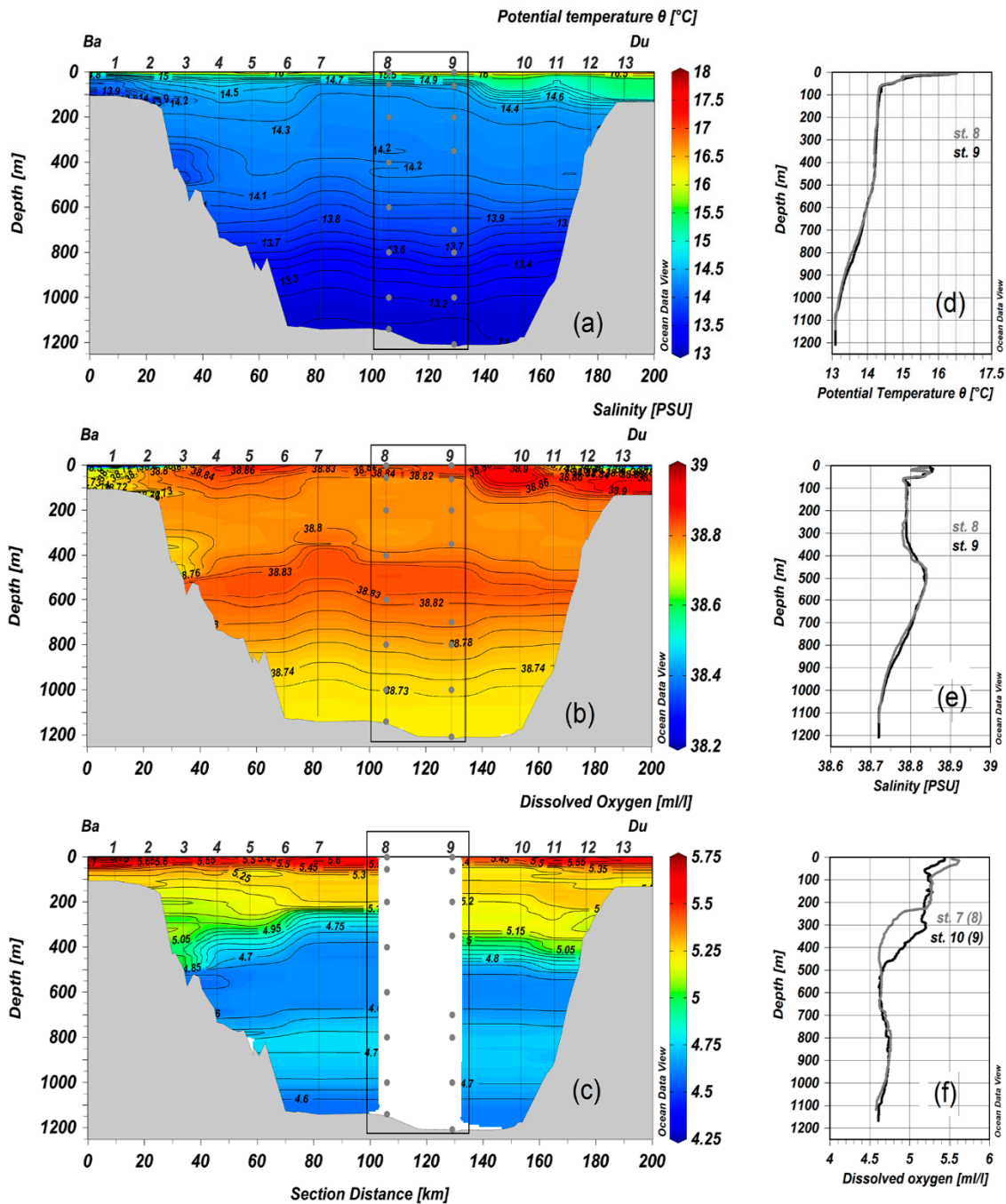


Figure 3. Vertical distribution of (a) potential temperature, (b) salinity, (c) dissolved oxygen, along the Bari-Dubrovnik (Ba-Du) section during the ESAW2 cruise in April 2016. Grey dots indicate locations of picoplankton sampling. Panels (d–f) show the vertical profiles of the same properties at stations 8 and 9, except the oxygen data, which were taken from stations 7 and 10 (data from station 8 and 9 are missing, due to technical problems).

In April 2016 (Figure 3), the largest differences with respect to the pre-winter conditions in December 2015 (Figure 2) were found mainly in the upper layer temperature, due to the season signal. The temperature differences between the western and eastern flanks, as well as between the surface and bottom layers over the western shelf, diminished with respect to December 2015 (Figure 3a). On the western slope, at depths between 300 and 500 m (stations 3 and 4), a branch of relatively cold, fresh, and ventilated water ($\theta \sim 14.10$ °C, $S \sim 38.74$, $DO \sim 4.9\text{--}5.1$ mL/L) pointed to a possible intrusion of northern and/or middle Adriatic waters. However, data collected in the deepest layers revealed that θ and DO did not change significantly with respect to the pre-winter period, while S values slightly increased from 38.72 to 38.74 (Figure 3d–f). At the two nearby stations, 8 and 9, the thermohaline properties were almost uniform. From the DO profiles at the stations 7 and 10 (close to 8 and 9, where DO values were not recorded due to technical problems), we might guess that the vertical convection and mixing, resulting in a homogenous vertical distribution of DO, reached 350 m at station 9, and 250 m at station 8. In any case, the vertical distribution of the physical parameters and DO (Figure 3) suggested that a weak vertical convection occurred during winter 2015–2016, and it probably did not exceed 400 m in depth, as confirmed by time-series data recorded at E2-M3A (<http://nettuno.ogs.trieste.it/e2-m3a/>), also located in the SAP (Figure 1). The highest S values (~ 38.94) measured in April 2016, associated with the LIW influence, were slightly lower than those observed in December 2015 (~ 38.95). From the physical parameters, we inferred that the doming structure, typical of the cyclonic circulation in the SAP, was much more enhanced in April than in December. Moreover, it was centered near station 7. This means that the sub-basin-scale cyclonic gyre was probably stronger in April than in December, favoring lateral exchanges along the perimeter of the SAP. The lateral exchange between both coastal flanks and the middle of the transect seemed less active with respect to December 2015. Biogeochemical properties were obtained through chemical analyses performed on water samples collected from discrete depths along the SAP transect. Here we reported the data from stations 8 and 9, relevant for the biological sampling (Figure 1). The vertical distribution of nutrients was similar at the two stations 8 and 9 (Figure 4), for both cruises. Nitrate, phosphates, and silicates were depleted in the upper layer and increased with increasing depth. Highest values of nitrates and phosphates were found between 400 and 600 m, whereas silicates increased almost uniformly until 800 m, and then more rapidly between 1000 m and 1100 m, reaching the highest values in the bottom waters, where turbidity (proportional to the suspended particle concentration) was also high (Figure S1a,c). Ammonia concentrations were higher in December 2015 than in April 2016. Nitrites were low, but local maxima were observed at depths between 50 and 100 m in both December and April, corresponding to fluorescence maxima (Figure S1b,d). The DON and DOP concentrations throughout the water column were higher in December 2015 than in April 2016 (Figure 5). On the contrary, DOC concentrations were higher in April 2016 than in December 2015 (Figure 5a,b). High concentrations of DOC, DON, and DOP were found in the upper layer, between the surface and 100 m. In the upper layer, at 100 m depth, turbidity was relatively high in both periods, with apparently higher values in April 2016 (Figure S1a,c). Turbidity slightly increased also between 200 m and 600 m, where a prominent LIW signal was found.

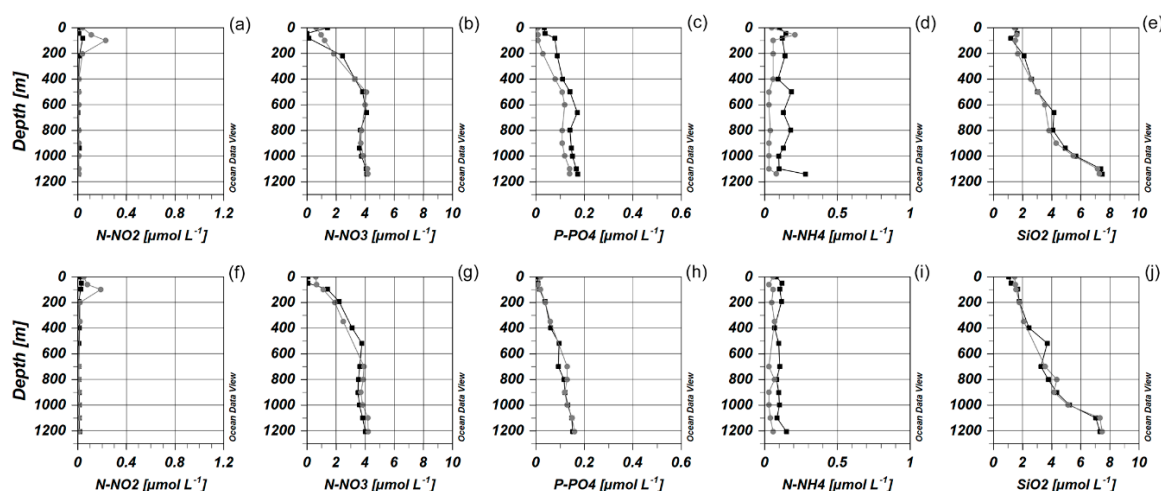


Figure 4. Vertical profiles of nutrients. Station 8: panels (a–e) and Station 9: panels (f–j). Periods: December 2015 ESAW1 (black line) and April 2016 ESAW2 (grey line). Symbols indicate sample locations.

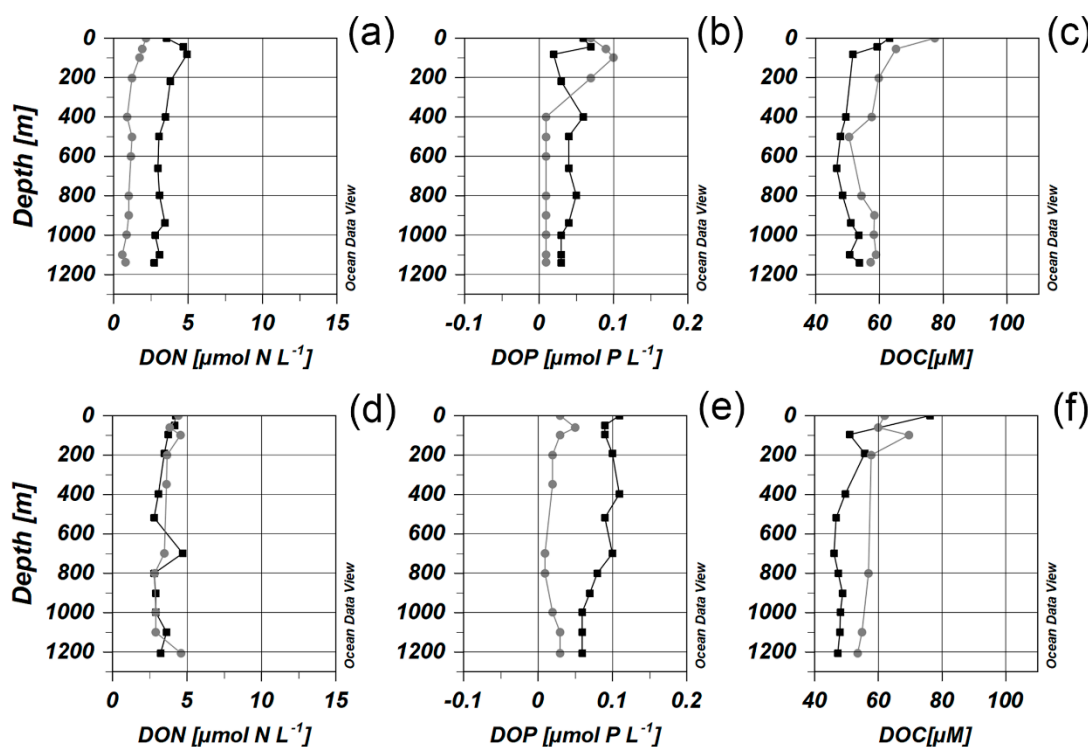


Figure 5. Vertical profiles of dissolved organic nitrogen (DON), dissolved organic phosphorus (DOP), and dissolved organic carbon (DOC). Station 8: panels (a–c). Station 9: panels (d–f). Periods: December 2015 ESAW1 (black line) and April 2016 ESAW2 (grey line). Symbols indicate sample locations.

3.2. Picoplankton Community

In both surveys, among the measured microbial community (heterotrophic bacteria, *Synechococcus*, *Prochlorococcus*, picoeukaryotes), *Synechococcus* abundances (Table S1) were the highest in the autotrophic fraction and reached values up to 93.93×10^3 cells mL^{-1} . *Prochlorococcus* and picoeukaryotes abundances were up to 47.09×10^3 cells mL^{-1} and 2.96×10^3 cells mL^{-1} , respectively. Bacterial abundance ranged from 0.03×10^6 to 0.24×10^6 cell mL^{-1} with the highest values found above 100 m depth.

In December, the autotrophic biomass (an average of $13.6 \mu\text{gCL}^{-1}$) was almost six times higher than heterotrophic (an average of $2.29 \mu\text{gCL}^{-1}$), with the domination of *Synechococcus*. Vertical distribution revealed the prevalence of autotrophic biomass over heterotrophic in the epipelagic

layer but also deep waters (Figure 6a,b). In April, the heterotrophic biomass was similar to that in December (on average $2.90 \mu\text{gCL}^{-1}$) and slightly higher than the autotrophic biomass (on average $2.47 \mu\text{gCL}^{-1}$). The autotrophic biomass, mainly composed by picoeukaryotes, was slightly higher than the heterotrophic biomass in the epipelagic layer, while in the deep waters, the heterotrophic biomass dominated among the observed communities (Figure 6c,d).

Bacterial production ranged from 0.01×10^4 to 0.09×10^4 cells $\text{h}^{-1} \text{mL}^{-1}$. The highest values were found at the surface, but surprisingly high values were recorded at 800 m and 1200 m depth, during April 2016 (Figure 7a). The ratio of nucleic acid content showed the domination of LNA cells in all samples within the bacterial community throughout the euphotic zone (up to 200 m) and the prevalence of HNA cells in the deeper layers (Figure 7b). The abundance of viruses ranged from 0.39×10^6 VLP mL^{-1} to 5.37×10^6 VLP mL^{-1} (Figure 7c). Overall, their vertical distribution revealed a large abundance in the euphotic zone and low abundance below 300 m depth, at both sampling sites. However, at both stations, values of VLP slightly increased in the layers below 800 m in December, while at station 8, also increased in the deep layer in April. The average virus to bacteria ratio (VBR) was higher in December (19 ± 10 at station 8 and 29 ± 12 at station 9) compared to April (8 ± 2 at station 8 and 8 ± 4 at station 9).

AAPs were observed in all samples during April, with abundance ranging from 0.04×10^4 to 0.61×10^4 cells mL^{-1} . In general, their vertical distribution showed similar patterns at both stations 8 and 9. Below 200 m, in correspondence of the nutricline and the minimum fluorescence layer (Figure S1b,d) the abundances of AAPs started decreasing steeply (Figure 7d). The proportion of AAPs abundances in total prokaryotes ranged from 0.65% to 2.48%, while the proportion of the AAPs biomass ranged from 0.37% to 4.09%, respectively.

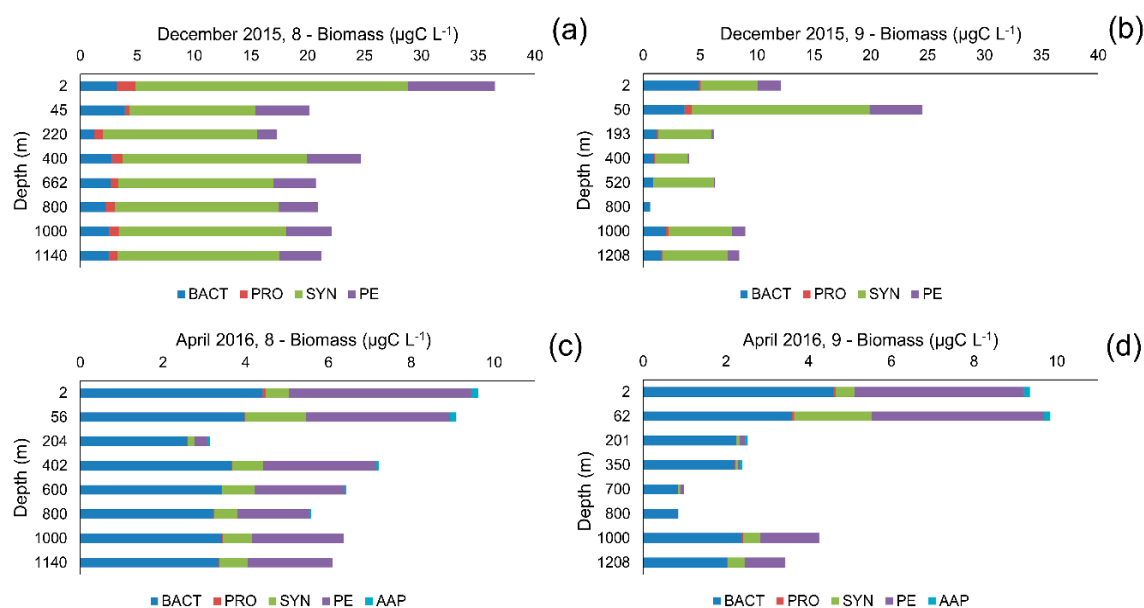


Figure 6. Vertical profiles of biomass for heterotrophic bacteria (BACT), *Prochlorococcus* (PRO), *Synechococcus* (SYN), picoeukaryotes (PE), aerobic anoxygenic phototrophs (AAP) at stations 8 (a) and 9 (b) in December 2015 (ESAW1) and at stations 8 (c) and 9 (d) in April 2016 (ESAW2).

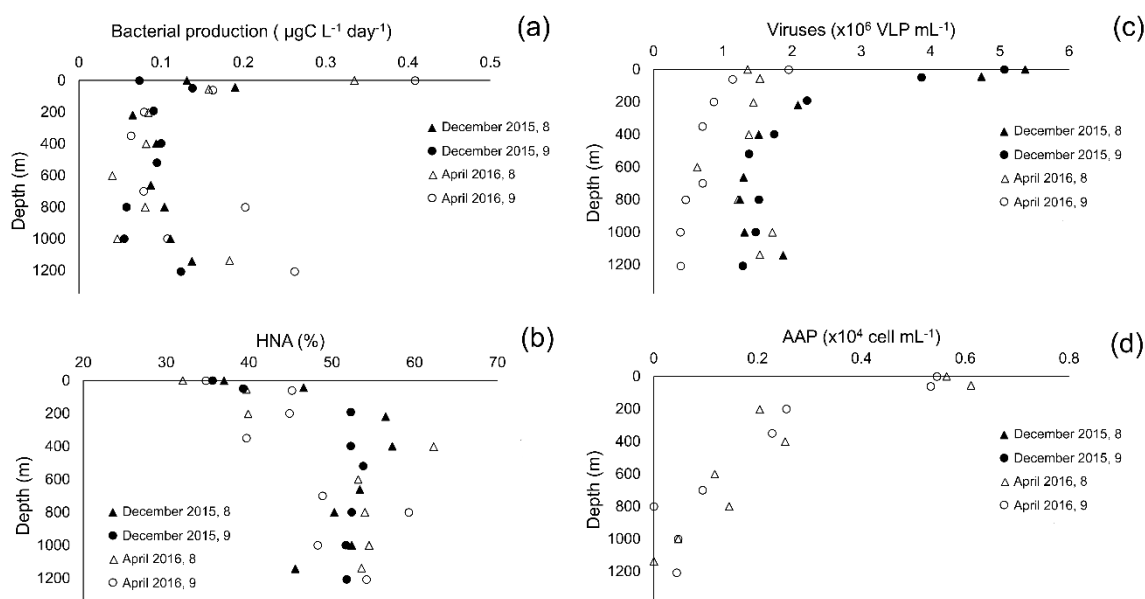


Figure 7. Vertical profile of bacterial production (a), HNA % (High Nucleic Acid content) (b), viruses (VLP) (c), and AAPs (d) at the station 8 and 9 in December 2015 (ESAW1) and in April 2016 (ESAW2).

3.3. Distribution of Picoplankton Community Members Concerning Environmental Variables

Relationship between environmental parameters and picoplankton was tested by Pearson's correlation analysis (Table S2). DOC, HNF, and temperature seemed to be the most important environmental factors for bacterial abundance and production, exhibiting significant positive correlations. Ammonium ion displayed a significant positive correlation with *Prochlorococcus* and *Synechococcus*. During the investigation period, VLP significantly correlated with autotrophic members of the picoplankton community.

Positive correlations of AAPs were found for temperature ($r = 0.83$; $p < 0.05$), for fluorescence ($r = 0.76$; $p < 0.05$), and for nitrites, nitrates, phosphates, and total dissolved phosphates ($r = 0.85$; $r = -0.94$; $r = -0.90$; $r = -0.69$; $n = 14$; $p < 0.05$). Furthermore, AAPs were also positively correlated with picoeukaryotes and HNF ($r = 0.74$; $r = 0.91$; $n = 14$; $p < 0.05$).

PCA ordination of picoplankton groups concerning environmental variables was used to analyze main factors affecting the abundances of the picoplankton groups (Figure 8a). PCA clustered the samples corresponding to depth (E-epipelagic layer; D-deep layer) and period (Figure 8b). The first principal component explained 44.83% of the variance and correlated positively with HNF and temperature, negatively with a concentration of nitrates and phosphates. The second principal component explained 17.75% of the variance and correlated positively with picoautotrophs and abundance of VLP (Table S3). Picoplankton community members were distributed in two groups, based on the correlation between them. On the one hand, bacteria, bacterial production, and LNA bacteria were closely related, while on the other hand, this was also the case for *Synechococcus* and *Prochlorococcus*. Bacterial cluster showed the strongest correlation with DOC, HNF, and temperature, as indicated by the perpendicular projection of bacterial arrow-tips on the line overlapping the DOC, HNF, and temperature arrow. Cyanobacteria were more related to ammonium, while HNA bacteria showed a positive relationship with nitrates and picoeukaryotes with VLP.

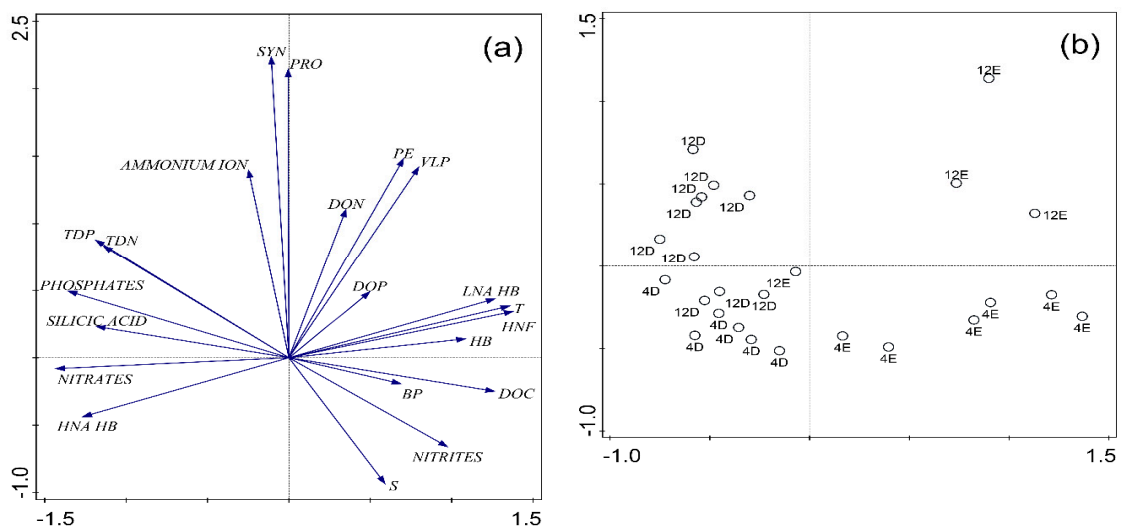


Figure 8. PCA (principal component analysis) of (a) biological (*Synechococcus*-SYN, *Prochlorococcus*-PRO, picoeukaryotes-PE, total bacteria—HB, HNA HB, LNA HB, VLP, HNF, bacterial production BP) and environmental parameters (Salinity—S, Temperature—T, nutrients). The arrow direction points out to the steepest increase of the variable. The angle between arrows indicates correlations between variables (an angle < 90° between two arrows of interest implies positive correlation), whereas the length of an arrow depicts the strength of association between a variable and the ordination axes shown in the biplot. (b) PCA clustering of the samples corresponding to depth (E-epipelagic layer; D-deep layer) and period. LNA: Low Nucleic Acid; VLP: virus-like particle; HNF: heterotrophic nanoflagellates.

The relationship between HNF as the main predator of bacteria and the bacteria was described by the Gasol model [46], which we used for our dataset. Most samples from the epipelagic layer were placed above the MRA line, whereas most samples from deep waters were below MRA. This pattern suggested a stronger coupling between bacteria and HNF in the epipelagic layer. In the deep waters layer, HNF predation pressure on bacteria was lower, suggesting larger importance for bottom-up control of bacteria and top-down control of HNF (Figure 9).

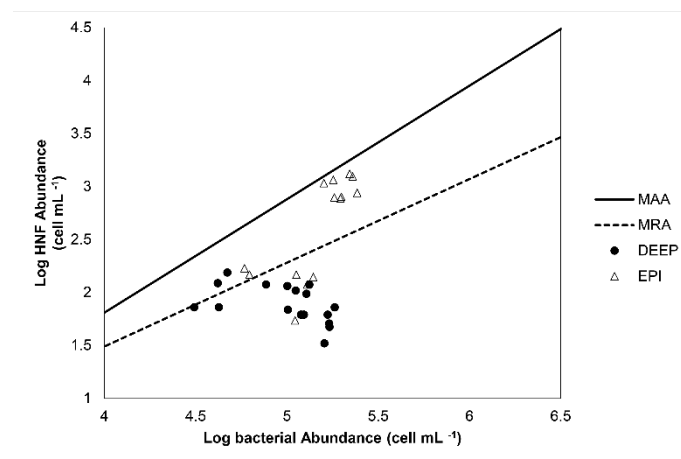


Figure 9. Relationship between bacterial and HNF abundance at study stations, plotted in a theoretical model (Gasol, 1994) (MAA-maximum attainable abundance: $\max \log \text{HNF} = -2.47 + 1.07 \log \text{bacterial abundance}$; MRA-mean realized abundance: $\text{mean} \log \text{HNF} = -1.67 + 0.79 \log \text{bacterial abundance}$) in epipelagic (epi-) and deep (deep-) water layers.

4. Discussion

One of the main findings in this survey was the unusually high biomass of picoautotrophs found in the epipelagic and deep layers in December 2015. *Synechococcus* dominated the picoplankton community with a maximum value of 23.95 μgCL^{-1} . Observed high value of *Synechococcus* biomass agrees with those measured in the Levantine basin during the late summer-autumn period [49]. It is well known that picophytoplankton tends to dominate autotrophic biomass and primary production in oligotrophic waters, like those of the Mediterranean Sea [50–52]. Furthermore, picoeukaryotes contributed significantly to the autotrophic biomass due to their larger size and carbon content, compared to cyanobacteria.

Physical and biogeochemical measurements performed in December 2015 revealed the presence of LIW in the intermediate layer and NAdDW at depths > 800 m. Our results also revealed the presence, in the deep layers of the SAP, of *Synechococcus*, *Prochlorococcus*, and picoeukaryotic cells coming from the Eastern Mediterranean and the North Adriatic Sea. Our findings agree well with previous studies [6,53], which associated the high abundances of *Synechococcus* and bacterial cells in the deep layers with water mass movement.

The results of this research showed the remarkably high autotrophic biomass in the deep waters, which is not characteristic of that environment. We suggest that picoautotrophs, aside from their important role in primary production, could be a significant carbon source for higher trophic levels in the form of dead or live prey, or as sinking particles in upper [54–58] and deep ocean waters [59]. In this study, physical and biogeochemical measurements performed in the Southern Adriatic revealed that weak vertical convection occurred during winter 2015–2016, which probably did not exceed 400 m depth. Moreover, a strong heterogeneity of the physical properties distribution, both horizontally and vertically, suggested the large influence of lateral exchanges due to the cyclonic circulation and mesoscale activity, apparently stronger during spring.

In April 2016, the picoplankton community throughout the water column was dominated by heterotrophic biomass (contrary to the December case), which is consistent with previous research for the open Adriatic area [3]. *Synechococcus*, *Prochlorococcus*, and picoeukaryotes abundances fluctuate in a range typical for the euphotic zone in the open Adriatic Sea [3,60,61]. In this survey, *Synechococcus* was the most abundant autotroph. *Synechococcus* hold the advantage over genus *Prochlorococcus* and thrive in P-depleted environments due to the high affinity for inorganic phosphorus and higher phosphate uptake rates as reported recently [62,63]. Furthermore, both genera of cyanobacteria showed a positive relationship with the concentration of ammonium, which is supported by the fact that *Synechococcus* can exploit both the reduced and the oxidized forms of nitrogen. In oligotrophic environments, ammonium represents the major nitrogen compound for primary production [64], and *Prochlorococcus* are effective in consuming the same [65,66].

Our findings clearly showed that bacterial production and biomass values measured in the deep waters were similar to the values for the epipelagic layer. La Ferla et al. [67] also found similar vertical patterns of bacterial density and bacterial production in the Western and the Eastern Mediterranean Sea. Additionally, we determined the dominance of HNA bacterial group in the deep-sea, while the LNA bacterial group prevailed in the epipelagic layer. Recent research from the Adriatic Sea pointed out the increase of HNA bacteria with depth, and together with LNA bacteria, they participated in the bacterial activity [10,68]. It is well known that HNA bacterial cells are larger than LNA cells and that the proportion of HNA bacteria increases with depth [69,70]. Larger cell size is reflected in a higher-level cell-specific activity or higher metabolic versatility in the mesopelagic ocean [5,70,71]. So, we argue that similar values of bacterial production measured in the deep water and epipelagic layer, together with the dominance of HNA bacteria in deep water, showed bacterial activity in the deep waters of SAP. We can conclude that the results of bacterial production as the measure of activity in this study support the idea that deep ocean prokaryotes are active as those living in the epipelagic waters [4,72–75]. Beside the domination of HNA cells in the bacterial community, our data showed increased values of DOC, phosphates, and bacterial production below 800 m during the post-winter period. This suggests

that the bacterial activity increases with the supply of organic carbon, as Nagata et al. [76] previously described for the deep-sea environment.

Bacterial abundance throughout the water column was approximately 10^5 cells mL^{-1} , which is per the recent data reported for the SAP [8,10] and with previous studies carried out in the Mediterranean Sea [67,72,77–79]. Heterotrophic bacteria contribute at a high percentage in total picoplankton biomass, acting as decomposers of organic matter and important producers of new biomass. Through grazing by HNF or larger zooplankton, their biomass becomes available to higher trophic levels, in both the epipelagic and deep waters of the Mediterranean Sea [5,46,59]. During our surveys, bacterial abundance and productivity showed positive relationships with DOC concentration and HNF abundance. Our results showed that the increase in bacterial abundance and cell production supported the increase in the number of HNF, especially in the epipelagic layer. It revealed that bacteria constitute a potential food resource for the nanoflagellate community and suggest a strong top-down control of bacteria. These results confirm previous findings showing [2,80] that predators prefer active bacteria and remove bacterial production, and that they can control the abundance of the bacterial community in surface waters [46]. Some studies [21,81] suggested strong bottom-up control of bacteria, which is in accordance with our results, showing a positive relationship between bacterial parameters and DOC concentration through the water column.

Little is known about the role and distribution of AAPs in the Adriatic Sea, especially in its deepest part. Šantić et al. [12] investigated AAPs abundances along the eastern Adriatic, in coastal and transitional waters, and found that their proportion in total prokaryotes was 7.3% ($\pm 4.3\%$). Celussi et al. [11] pointed out that the concentration of bacteriochlorophyll *a*, the main pigment of AAPs, could be converted into abundance. Therefore, AAPs might represent up to 10% of total prokaryotes in the open Adriatic Sea. In recent research of AAPs, the abundance, the proportion in total prokaryotes, and biomass decreased along the trophic gradient [45]. Furthermore, these counts were substantially low at the oligotrophic open sea station, especially under 70 m depth. Similar vertical distribution was already noted [13,82–86] since these organisms inhabit the euphotic zone because of their phototrophic nature. The results of this study are consistent with previous reports, which also found lower abundances in the more oligotrophic area when compared to the more productive regions or shelf seas [13,39,82,85–89].

The main environmental parameters that influenced the picoplankton community according to the research conducted by Šantić et al. [12] were chlorophyll, followed by nitrates and temperature.

In this research, fluorescence, as a proxy of chlorophyll, nitrates, nitrites, phosphates, and total dissolved phosphates, influenced the abundance of AAPs. Besides, the correlation found between bacteria and AAPs, which has also been reported by Celussi et al. [11], could be explained by the fact that both AAPs and heterotrophic bacteria rely on labile DOC, part of which is released by phytoplankton. Secondly, AAPs and phytoplankton have a similar dependence on light [90], and this relationship may reflect the same dependence on limiting nutrients, such as phosphorus or nitrogen [15]. The majority of AAP surveys have shown that temperature, salinity, chlorophyll concentration, and carbon and nitrogen compounds affect the dynamics and distribution of the AAP population [39,85–87,89]. The high positive correlation between AAPs and HNF found during our study suggest that AAPs represent an important prey for flagellates in the open Adriatic Sea, as documented in the Mediterranean Sea [91,92]. It is a well-known fact that AAPs are larger than the average heterotrophic bacteria [13,14,86,93] and that, consequently, their biomass contribution to total bacterial biomass is also high (up to 11% in this survey). Cell size is an important parameter in feeding ecology, which provides a valuable insight into the trophic significance of AAPs. It was previously observed that nanoflagellates preferentially ingest the larger bacterial cells [94–96].

The number of viruses ranged between 0.39×10^6 VLP MI^{-1} and 5.37×10^6 VLP mL^{-1} , which is in accordance with other studies for the Adriatic and Mediterranean Sea [97–101]. Their average abundance was $16 \pm 12\times$ higher than the abundance of prokaryotes, as well as in previous studies on oligotrophic deep waters [99]. Relatively high VBR determined in the deep waters could be a result

of higher lytic activity caused by lysogenic viruses. Water mass sinking to the SAP could cause the induction of lysogenic viruses and thus keep the viral abundance stable. Winter et al. [102] recently pointed out that mixing in the deeper waters led to the induction of lysogenic viruses. Viruses positively correlated with the members of the picoplankton community at the sampling sites, indicating their involvement in shaping the picoplankton abundances in the oligotrophic waters of the SAP. The PCA analysis revealed a close relationship between viruses and the picoautotrophic group. It is known that viruses can be an important mortality factor for picoeukaryotes in oligotrophic oceanic waters [103]. Our results suggest that viruses are an important component of the microbial food web, but this topic should be addressed in further studies.

5. Conclusions

The present study points out the importance of *Synechococcus*, *Prochlorococcus*, picoeukaryotes, heterotrophic bacteria, AAPs, heterotrophic nanoflagellates, and viruses altogether in the carbon flux through the microbial food web in the SAP for the first time, which depended largely on water mass movements and mixing.

A significant amount of picoautotrophic biomass was found in the epipelagic, as well as in the deep layers, during the period under the influence of LIW inflow and NAdDW sinking, respectively. After weak vertical convection during winter, heterotrophic bacteria dominated picoplankton biomass throughout the water column. Furthermore, bacterial activity values in the deep layer were similar to the ones obtained in the epipelagic layer. Besides the physical pump, the changes in the picoplankton community in the SAP were mainly driven by nutrient availability, more specifically bacteria by DOC and cyanobacteria by ammonium ion. Our results also reveal that bacteria represent an important prey for nanoflagellates, especially in the epipelagic layer. Moreover, autotrophic and heterotrophic members of the picoplankton community could be available prey and a source of carbon for the food web below the epipelagic layer. Finally, AAPs contributed up to 4% of bacterial biomass, which can be transferred through higher trophic levels by grazing. Viral lysis may affect the activity of the picoplankton community and serve as an important source of DOC in the deep-sea.

Supplementary Materials: The following are available online at <http://www.mdpi.com/2073-4441/11/8/1655/s1>, Figure S1: Vertical profiles of optical backscattering and fluorescence. Station 8: panels (a) and (b). Station 9: panels (c) and (d). Periods: December 2015 ESAW1 (black line) and April 2016 ESAW2 (grey line), Table S1: Summary of the picoplankton community abundances, Table S2. Summary of the correlations between picoplankton community (*Synechococcus*-SYN, *Prochlorococcus*-PRO, picoeukaryotes-PE, total bacteria HB, HNA HB, LNA HB, VLP, HNF, bacterial production BP) and environmental variables (Temperature-T, nutrients). Acronym n.s. stands for not significant, Table S3. Summary of the principal component analysis (PCA) of the picoplankton groups and environmental variables.

Author Contributions: Conceptualization, M.B.; Data curation, V.K.; Formal analysis, D.Š. and A.V.T.; Funding acquisition, V.K.; Investigation, D.Š.; Methodology, D.Š., M.G., A.V.T., M.O., C.S., S.Š. and B.G.; Project administration, V.K.; Supervision, M.Š.; Writing—original draft, D.Š.; Writing—review and editing, V.K., M.B., M.G., A.V.T. and M.O.

Funding: The study was carried out within the framework of the EUROFLEETS2 research infrastructures project under the 7th Framework Program of the European Commission (grant agreement 312762). It was partially funded by the Italian national project RITMARE (Ricerca Italiana per il Mare, grant numbers: SP3-WP3-AZ1; SP4-LI4-WP1; SP5-WP3-AZ3) and by the Croatian Science Foundation as a part of research projects: IP-2014-09-4143 “Marine microbial food web processes in global warming perspective” (MICROGLOB).

Acknowledgments: We thank L.U. for nutrients, TDN and TDP analyses, H.M. and S.M. for their help with sampling, and the crew of R/V BIOS DVA.

Conflicts of Interest: The authors declare no conflict of interest.

References

- Ninčević Gladan, Ž.; Marasović, I.; Kušpilić, G.; Krstulović, N.; Šolić, M.; Šestanović, S. Abundance and composition of picoplankton in the mid Adriatic Sea. *Acta Adriat.* **2006**, *47*, 127–140.
- Šolić, M.; Grbec, B.; Matić, F.; Šantić, D.; Šestanović, S.; Gladan, Ž.N.; Bojanić, N.; Ordulj, M.; Jozić, S.; Vrdoljak, A. Spatio-temporal reproducibility of the microbial food web structure associated with the change in temperature: Long-term observations in the Adriatic Sea. *Prog. Oceanogr.* **2018**, *161*, 87–101. [[CrossRef](#)]
- Šantić, D.; Krstulović, N.; Šolić, M.; Ordulj, M.; Kušpilić, G. Dynamics of prokaryotic picoplankton community in the central and southern Adriatic Sea (Croatia). *Helgoland Mar. Res.* **2013**, *67*, 471–481. [[CrossRef](#)]
- Tanaka, T.; Rassoulzadegan, F. Full-depth profile (0–2000m) of bacteria, heterotrophic nanoflagellates and ciliates in the NW Mediterranean Sea: Vertical partitioning of microbial trophic structures. *Deep Sea Res. Part II Top. Stud. Oceanogr.* **2002**, *49*, 2093–2107. [[CrossRef](#)]
- Aristegui, J.; Gasol, J.M.; Duarte, C.M.; Herndl, G.J. Microbial oceanography of the dark ocean's pelagic realm. *Limnol. Oceanogr.* **2009**, *54*, 1501–1529. [[CrossRef](#)]
- Vilibić, I.; Šantić, D. Deep water ventilation traced by *Synechococcus* cyanobacteria. *Ocean Dyn.* **2008**, *58*, 119–125. [[CrossRef](#)]
- Azzaro, M.; La Ferla, R.; Maimone, G.; Monticelli, L.S.; Zaccone, R.; Civitarese, G. Prokaryotic dynamics and heterotrophic metabolism in a deep convection site of Eastern Mediterranean Sea (the Southern Adriatic Pit). *Cont. Shelf Res.* **2012**, *44*, 106–118. [[CrossRef](#)]
- Batistić, M.; Jasprica, N.; Carić, M.; Čalić, M.; Kovačević, V.; Garić, R.; Njire, J.; Mikuš, J.; Bobanović-Čolić, S. Biological evidence of a winter convection event in the South Adriatic: A phytoplankton maximum in the aphotic zone. *Cont. Shelf Res.* **2012**, *44*, 57–71. [[CrossRef](#)]
- Cerino, F.; Aubry, F.B.; Coppola, J.; La Ferla, R.; Maimone, G.; Socal, G.; Totti, C. Spatial and temporal variability of pico-, nano- and microphytoplankton in the offshore waters of the southern Adriatic Sea (Mediterranean Sea). *Cont. Shelf Res.* **2012**, *44*, 94–105. [[CrossRef](#)]
- Šilović, T.; Mihanović, H.; Batistić, M.; Radić, I.D.; Hrustić, E.; Najdek, M. Picoplankton distribution influenced by thermohaline circulation in the southern Adriatic. *Cont. Shelf Res.* **2018**, *155*, 21–33. [[CrossRef](#)]
- Celussi, M.; Gallina, A.A.; Ras, J.; Giani, M.; Del Negro, P. Effect of sunlight on prokaryotic organic carbon uptake and dynamics of photoheterotrophy in the Adriatic Sea. *Aquat. Microb. Ecol.* **2015**, *74*, 235–249. [[CrossRef](#)]
- Šantić, D.; Šestanović, S.; Vrdoljak, A.; Šolić, M.; Kušpilić, G.; Ninčević Gladan, Ž.; Koblížek, M. Distribution of aerobic anoxygenic phototrophs in the Eastern Adriatic Sea. *Mar. Environ. Res.* **2017**, *130*, 134–141. [[CrossRef](#)] [[PubMed](#)]
- Sieracki, M.E.; Gilg, I.C.; Thier, E.C.; Poulton, N.J.; Goericke, R. Distribution of planktonic aerobic anoxygenic photoheterotrophic bacteria in the northwest Atlantic. *Limnol. Oceanogr.* **2006**, *51*, 38–46. [[CrossRef](#)]
- Stegman, M.R.; Cottrell, M.T.; Kirchman, D.L. Leucine incorporation by aerobic anoxygenic phototrophic bacteria in the Delaware estuary. *ISME J.* **2014**, *8*, 2339–2348. [[CrossRef](#)] [[PubMed](#)]
- Koblížek, M. Ecology of aerobic anoxygenic phototrophs in aquatic environments. *FEMS Microbiol. Rev.* **2015**, *39*, 854–870. [[CrossRef](#)]
- Kovačević, V.; Gačić, M.; Poulain, P.M. Eulerian current measurements in the Strait of Otranto and in the Southern Adriatic. *J. Mar. Syst.* **1999**, *20*, 255–278. [[CrossRef](#)]
- Yari, S.; Kovačević, V.; Cardin, V.; Gačić, M.; Bryden, H.L. Direct estimate of water, heat, and salt transport through the Strait of Otranto. *J. Geophys. Res. Oceans* **2012**, *117*. [[CrossRef](#)]
- Artegiani, A.; Paschini, E.; Russo, A.; Bregant, D.; Raicich, F.; Pinardi, N. The Adriatic Sea General Circulation. Part I: Air-Sea Interactions and Water Mass Structure. *J. Phys. Oceanogr.* **1997**, *27*, 1492–1514. [[CrossRef](#)]
- Buljan, M. Oceanographical properties of the Adriatic Sea. *Oceanogr. Mar. Biol. Ann. Rev.* **1976**, *14*, 11–98.
- Vukadin, I.; Stojanoski, L. Phosphorus versus nitrogen limitation in the middle Adriatic Sea. In Proceedings of the Rapport du 36e Congrès de la Commission Internationale pour l'Exploration Scientifique de la mer Méditerranée, Monaco, 1 October 2001.
- Šolić, M.; Krstulović, N.; Vilibić, I.; Kušpilić, G.; Šestanović, S.; Šantić, D.; Ordulj, M. The role of water mass dynamics in controlling bacterial abundance and production in the middle Adriatic Sea. *Mar. Environ. Res.* **2008**, *65*, 388–404. [[CrossRef](#)]

22. Skejić, S.; Arapov, J.; Kovačević, V.; Bužančić, M.; Bensi, M.; Giani, M.; Bakrač, A.; Mihanović, H.; Ninčević Gladan, Ž.; Urbini, L.; et al. Coccolithophore diversity in open waters of the middle Adriatic Sea in pre-and post-winter periods. *Mar. Micropaleontol.* **2018**, *43*, 30–45. [[CrossRef](#)]
23. Gačić, M.; Borzelli, G.L.E.; Civitarese, G.; Cardin, V.; Yari, S. Can internal processes sustain reversals of the ocean upper circulation? The Ionian Sea example. *Geophys. Res. Lett.* **2010**, *37*, L09608. [[CrossRef](#)]
24. Bensi, M.; Velaoras, D.; Meccia, L.V.; Cardin, V. Effects of the Eastern Mediterranean Sea circulation on the thermohaline properties as recorded by fixed deep-ocean observatories. *Deep Sea Res. Part I Oceanogr. Res. Pap.* **2016**, *112*, 1–13. [[CrossRef](#)]
25. Civitarese, G.; Gačić, M.; Lipizer, M.; Eusebi Borzelli, G.L. On the impact of the Bimodal Oscillating System (BiOS) on the biogeochemistry and biology of the Adriatic and Ionian Seas (Eastern Mediterranean). *Biogeosciences* **2010**, *7*, 3987–3997. [[CrossRef](#)]
26. Batistić, M.; Garić, R.; Molinero, J.C. Interannual variations in Adriatic Sea zooplankton mirror shifts in circulation regimes in the Ionian Sea. *Clim. Res.* **2014**, *61*, 231–240. [[CrossRef](#)]
27. Matić, F.; Kovač, Ž.; Vilibić, I.; Mihanović, H.; Morović, M.; Grbec, B.; Leder, N.; Džoić, T. Oscillating Adriatic temperature and salinity regimes mapped using the Self-Organizing Maps method. *Cont. Shelf Res.* **2017**, *132*, 11–18. [[CrossRef](#)]
28. Vilibić, I.; Orlić, M. Adriatic water masses, their rates of formation and transport through the Otranto Strait. *Deep Sea Res. Part I Oceanogr. Res. Pap.* **2002**, *49*, 1321–1340. [[CrossRef](#)]
29. Querin, S.; Bensi, M.; Cardin, V.; Solidoro, C.; Bacer, S.; Mariotti, L.; Stel, F.; Malačić, V. Saw-tooth modulation of the deep-water thermohaline properties in the southern Adriatic Sea. *J. Geophys. Res. Oceans* **2016**, *121*, 4585–4600. [[CrossRef](#)]
30. Vilibić, I.; Orlić, M. Least-squares tracer analysis of water masses in the South Adriatic (1967–1990). *Deep Sea Res. Part I Oceanogr. Res. Pap.* **2001**, *48*, 2297–2330. [[CrossRef](#)]
31. Cardin, V.; Bensi, M.; Pacciaroni, M. Variability of water mass properties in the last two decades in the Southern Adriatic Sea with emphasis on the period 2006–2009. *Cont. Shelf Res.* **2011**, *31*, 951–965. [[CrossRef](#)]
32. Bensi, M.; Cardin, V.; Rubino, A.; Notarstefano, G.; Poulain, P.M. Effects of winter convection on the deep layer of the Southern Adriatic Sea in 2012. *J. Geophys. Res. Oceans* **2013**, *118*, 6064–6075. [[CrossRef](#)]
33. Schlitzer, R.; Roether, W.; Oster, H.; Junghans, H.; Hausmann, M.; Johannsen, H.; Michelato, A. Chlorofluoromethane and oxygen in the Eastern Mediterranean. *Deep Sea Res. Part A Oceanogr. Res. Pap.* **1991**, *38*, 1531–1535. [[CrossRef](#)]
34. Mihanović, H.; Vilibić, I.; Carniel, S.; Tudor, M.; Russo, A.; Bergamasco, A.; Bubić, N.; Ljubešić, Z.; Viličić, D.; Boldrin, A.; et al. Exceptional dense water formation on the Adriatic shelf in the winter of 2012. *Ocean Sci.* **2013**, *9*, 561–572. [[CrossRef](#)]
35. Schlitzer, R. Ocean Data View. 2018. Available online: <http://odv.awi.de/> (accessed on 1 February 2019).
36. Hansen, H.P.; Koroleff, F. Determination of nutrients. *Methods Seawater Anal.* **1999**, *27*, 159–228.
37. Marie, D.; Partensky, F.; Jacquet, S.; Vaulot, D. Enumeration and cell cycle analysis of natural populations of marine picoplankton by flow cytometry using the nucleic acid stain SYBR Green I. *Appl. Environ. Microbiol.* **1997**, *63*, 186–193. [[PubMed](#)]
38. Christaki, U.; Courties, C.; Massana, R.; Catala, P.; Lebaron, P.; Gasol, J.M.; Zubkov, M.V. Optimized routine flow cytometric enumeration of heterotrophic flagellates using SYBR Green I. *Limnol. Oceanogr. Methods* **2011**, *9*, 329–339. [[CrossRef](#)]
39. Mašín, M.; Zdun, A.; Ston-Egiert, J.; Nausch, M.; Labrenz, M.; Moulisová, V.; Koblížek, M. Seasonal changes and diversity of aerobic anoxygenic phototrophs in the Baltic Sea. *Aquat. Microb. Ecol.* **2006**, *45*, 247–254. [[CrossRef](#)]
40. Noble, R.T.; Fuhrman, J.A. Use of SYBR Green I for rapid epifluorescence counts of marine viruses and bacteria. *Aquat. Microb. Ecol.* **1998**, *14*, 113–118. [[CrossRef](#)]
41. Fuhrman, J.A.; Azam, F. Thymidine incorporation as a measure of heterotrophic bacterioplankton production in marine surface waters: Evaluation and field results. *Mar. Biol.* **1982**, *66*, 109–120. [[CrossRef](#)]
42. Lee, S.; Fuhrman, J.A. Relationships between biovolume and biomass of naturally derived marine bacterioplankton. *Appl. Environ. Microbiol.* **1987**, *53*, 1298–1303.
43. Kirchman, D.L. *Handbook of Methods in Aquatic Microbial Ecology*; Lewis Publishers: Boca Raton, FL, USA, 1993; pp. 509–512.

44. Buitenhuis, E.T.; Li, W.K.W.; Vaulot, D.; Lomas, M.W.; Landry, M.R.; Partensky, F.; McManus, G.B. Picophytoplankton biomass distribution in the global ocean. *Earth Syst. Sci. Data* **2012**, *4*, 37–46. [[CrossRef](#)]
45. Vrdoljak Tomaš, A.; Šantić, D.; Šolić, M.; Ordulj, M.; Jozić, S.; Šestanović, S.; Matić, F.; Kušpilić, G.; Ninčević Gladan, Ž. Dynamics of Aerobic Anoxygenic Phototrophs along the trophic gradient in the central Adriatic Sea. *Deep Sea Res. Part II Top. Stud. Oceanogr.* **2019**. [[CrossRef](#)]
46. Gasol, J.M. A framework for the assessment of top-down vs bottom-up control of heterotrophic nanoflagellate abundance. *Mar. Ecol. Prog. Ser.* **1994**, *113*, 291–300. [[CrossRef](#)]
47. ter Braak, C.J.; Šmilauer, P. *Canoco Reference Manual and User's Guide: Software for Ordination*, version 5.0; Microcomputer Power: Ithaca, NY, USA, 2012.
48. Rubino, A.; Romanenkov, D.; Zanchettin, D.; Cardin, V.; Hainbucher, D.; Bensi, M.; Boldrin, A.; Langone, L.; Miserocchi, S.; Turchetto, M. On the descent of dense water on a complex canyon system in the southern Adriatic basin. *Cont. Shelf Res.* **2012**, *44*, 20–29. [[CrossRef](#)]
49. Bayindirli, C.; Ulysal, Z. Monthly changes in the abundance and biomass of cyanobacteria *Synechococcus* in the Cilician Basin. *Rapp. Comm. Int. Mer. Médit.* **2007**, *38*, 347.
50. Li, W.K. Annual average abundance of heterotrophic bacteria and *Synechococcus* in surface ocean waters. *Limnol. Oceanogr.* **1998**, *43*, 1746–1753. [[CrossRef](#)]
51. Zubkov, M.V.; Sleigh, M.A.; Burkill, P.H.; Leakey, R.J. Picoplankton community structure on the Atlantic Meridional Transect: A comparison between seasons. *Prog. Oceanogr.* **2000**, *45*, 369–386. [[CrossRef](#)]
52. Li, W.K.W.; Harrison, W.G. Chlorophyll, bacteria and picophytoplankton in ecological provinces of the North Atlantic. *Deep Sea Res. Part II Top. Stud. Oceanogr.* **2001**, *48*, 2271–2293. [[CrossRef](#)]
53. Carlucci, A.F.; Craven, D.B.; Robertson, K.J.; Henrichs, S.M. Microheterotrophic utilization of dissolved free amino-acids in depth profiles of southern-California borderland basin waters. *Oceanol. Acta* **1986**, *9*, 89–96.
54. DeLong, E.F.; Yayanos, A.A. Biochemical function and ecological significance of novel bacterial lipids in deep-sea prokaryotes. *Appl. Environ. Microbiol.* **1986**, *51*, 730–737.
55. Li, W.K. Primary production of prochlorophytes, cyanobacteria, and eukaryotic ultraphytoplankton: Measurements from flow cytometric sorting. *Limnol. Oceanogr.* **1994**, *39*, 169–175. [[CrossRef](#)]
56. Partensky, F.; Blanchot, J.; Lantoiné, F.; Neveux, J.; Marie, D. Vertical structure of picophytoplankton at different trophic sites of the tropical northeastern Atlantic Ocean. *Deep Sea Res. Part I Oceanogr. Res. Pap.* **1996**, *43*, 1191–1213. [[CrossRef](#)]
57. Blanchot, J.; André, J.M.; Navarette, C.; Neveux, J.; Radenac, M.H. Picophytoplankton in the equatorial Pacific: Vertical distributions in the warm pool and in the high nutrient low chlorophyll conditions. *Deep Sea Res. Part I Oceanogr. Res. Pap.* **2001**, *48*, 297–314. [[CrossRef](#)]
58. Buesseler, K.O.; Lamborg, C.H.; Boyd, P.W.; Lam, P.J.; Trull, T.W.; Bidigare, R.R.; Bishop, J.K.; Casciotti, K.L.; Dehairs, F.; Elskens, M.; et al. Revisiting carbon flux through the ocean's twilight zone. *Science* **2007**, *316*, 567–570. [[CrossRef](#)] [[PubMed](#)]
59. Zhang, Y.; Jiao, N.; Hong, N. Comparative study of picoplankton biomass and community structure in different provinces from subarctic to subtropical oceans. *Deep Sea Res. Part II Top. Stud. Oceanogr.* **2008**, *55*, 1605–1614. [[CrossRef](#)]
60. Šilović, T.; Balagué, V.; Orlić, S.; Pedrós-Alió, C. Picoplankton seasonal variation and community structure in the northeast Adriatic coastal zone. *FEMS Microbiol. Ecol.* **2012**, *82*, 678–691. [[CrossRef](#)] [[PubMed](#)]
61. Najdek, M.; Paliaga, P.; Šilović, T.; Batistić, M.; Garić, R.; Supić, N.; Ivančić, I.; Ljubimir, S.; Korlević, M.; Jasprica, N.; et al. Picoplankton community structure before, during and after convection event in the offshore waters of the Southern Adriatic Sea. *Biogeosciences* **2014**, *11*, 2645–2659. [[CrossRef](#)]
62. Moutin, T.; Thingstad, T.F.; Van Wambeke, F.; Marie, D.; Slawyk, G.; Raimbault, P.; Claustre, H. Does competition for nanomolar phosphate supply explain the predominance of the cyanobacterium *Synechococcus*? *Limnol. Oceanogr.* **2002**, *47*, 1562–1567. [[CrossRef](#)]
63. Martiny, A.C.; Kathuria, S.; Berube, P.M. Widespread metabolic potential for nitrite and nitrate assimilation among Prochlorococcus ecotypes. *Proc. Natl. Acad. Sci. USA* **2009**, *106*, 10787–10792. [[CrossRef](#)]
64. Raven, J.A.; Wollenweber, B.; Handley, L.L. A comparison of ammonium and nitrate as nitrogen sources for photolithotrophs. *New Phytol.* **1992**, *121*, 19–32. [[CrossRef](#)]
65. Partensky, F.; Hess, W.R.; Vaulot, D. *Prochlorococcus*, a marine photosynthetic prokaryote of global significance. *Microbiol. Mol. Biol. Rev.* **1999**, *63*, 106–127. [[PubMed](#)]

66. Wyman, M.; Bird, C. Lack of control of nitrite assimilation by ammonium in an oceanic picocyanobacterium, *Synechococcus* sp. strain WH 8103. *Appl. Environ. Microbiol.* **2007**, *73*, 3028–3033. [[CrossRef](#)] [[PubMed](#)]
67. La Ferla, R.; Azzaro, M.; Budillon, G.; Caroppo, C.; Decembrini, F.; Maimone, G. Distribution of the prokaryotic biomass and community respiration in the main water masses of the Southern Tyrrhenian Sea (June and December 2005). *Adv. Ocean. Limnol.* **2010**, *1*, 235–257. [[CrossRef](#)]
68. Šantić, D.; Krstulović, N.; Šolić, M.; Kušpilić, G. HNA and LNA bacteria in relation to the activity of heterotrophic bacteria. *Acta Adriat.* **2012**, *53*, 25–40.
69. Andrade, L.; Gonzalez, A.M.; Araujo, F.V.; Paranhos, R. Flow cytometry assessment of bacterioplankton in tropical marine environments. *J. Microbiol. Methods* **2003**, *55*, 841–850. [[CrossRef](#)] [[PubMed](#)]
70. Corzo, A.; Rodríguez-Gálvez, S.; Lubian, L.; Sobrino, C.; Sangrá, P.; Martínez, A. Antarctic marine bacterioplankton subpopulations discriminated by their apparent content of nucleic acids differ in their response to ecological factors. *Polar Biol.* **2005**, *29*, 27–39. [[CrossRef](#)]
71. Reinthaler, T.; Van Aken, H.; Veth, C.; Arístegui, J.; Robinson, C.; Williams, P.J.L.B.; Lebaron, P.; Herndl, G.J. Prokaryotic respiration and production in the meso- and bathypelagic realm of the eastern and western North Atlantic basin. *Limnol. Oceanogr.* **2006**, *51*, 1262–1273. [[CrossRef](#)]
72. Tanaka, T.; Rassoulzadegan, F. Vertical and seasonal variations of bacterial abundance and production in the mesopelagic layer of the NW Mediterranean Sea: bottom-up and top-down controls. *Deep Sea Res. Part I Oceanogr. Res. Pap.* **2004**, *51*, 531–544. [[CrossRef](#)]
73. Herndl, G.J.; Reinthaler, T.; Teira, E.; van Aken, H.; Veth, C.; Pernthaler, A.; Pernthaler, J. Contribution of Archaea to total prokaryotic production in the deep Atlantic Ocean. *Appl. Environ. Microb.* **2005**, *71*, 2303–2309. [[CrossRef](#)]
74. Teira, E.; Van Aken, H.; Veth, C.; Herndl, G.J. Archaeal uptake of enantiomeric amino acids in the meso- and bathypelagic waters of the North Atlantic. *Limnol. Oceanogr.* **2006**, *51*, 60–69. [[CrossRef](#)]
75. Del Giorgio, P.A.; Gasol, J.M. Physiological structure and single-cell activity in marine bacterioplankton. In *Microbial Ecology of the Oceans*, 2nd ed.; Kirchman, D.L., Ed.; John Wiley & Sons, Inc.: New York, NY, USA, 2008; pp. 243–285.
76. Nagata, T.; Fukuda, H.; Fukuda, R.; Koike, I. Bacterioplankton distribution and production in deep Pacific waters: Large-scale geographic variations and possible coupling with sinking particle fluxes. *Limnol. Oceanogr.* **2000**, *45*, 426–435. [[CrossRef](#)]
77. Tholosan, O.; Garcin, J.; Bianchi, A. Effects of hydrostatic pressure on microbial activity through a 2000 m deep water column in the NW Mediterranean Sea. *Mar. Ecol. Prog. Ser.* **1999**, *183*, 49–57. [[CrossRef](#)]
78. La Ferla, R.; Azzaro, M.; Caruso, G.; Monticelli, L.S.; Maimone, G.; Zaccone, R.; Packard, T.T. Prokaryotic abundance and heterotrophic metabolism in the deep Mediterranean Sea. *Adv. Oceanogr. Limnol.* **2010**, *1*, 143–166. [[CrossRef](#)]
79. Yokokawa, T.; De Corte, D.; Sintes, E.; Herndl, G.J. Spatial patterns of bacterial abundance, activity and community composition in relation to water masses in the eastern Mediterranean Sea. *Aquat. Microb. Ecol.* **2010**, *59*, 185–195. [[CrossRef](#)]
80. Del Giorgio, P.A.; Gasol, J.M.; Vaqué, D.; Mura, P.; Agustí, S.; Duarte, C.M. Bacterioplankton community structure: Protists control net production and the proportion of active bacteria in a coastal marine community. *Limnol. Oceanogr.* **1996**, *41*, 1169–1179. [[CrossRef](#)]
81. Šolić, M.; Krstulović, N.; Kušpilić, G.; Gladan, Ž.N.; Bojanić, N.; Šestanović, S.; Šantić, D.; Ordulj, M. Changes in microbial food web structure in response to changed environmental trophic status: A case study of the Vranjic Basin (Adriatic Sea). *Mar. Environ. Res.* **2010**, *70*, 239–249. [[CrossRef](#)] [[PubMed](#)]
82. Cottrell, M.T.M.; Mannino, A.; Kirchman, D.L. Aerobic anoxygenic phototrophic bacteria in the Mid-Atlantic Bight and the North Pacific Gyre. *Appl. Environ. Microbiol.* **2006**, *72*, 557–564. [[CrossRef](#)] [[PubMed](#)]
83. Lami, R.; Cottrell, M.; Ras, J.; Ulloa, O.; Obernosterer, I.; Claustre, H.; Kirchman, D.L.; Lebaron, P. High abundances of aerobic anoxygenic photosynthetic bacteria in the South Pacific Ocean. *Appl. Environ. Microbiol.* **2007**, *73*, 4198–4205. [[CrossRef](#)] [[PubMed](#)]
84. Lami, R.; Čuperová, Z.; Ras, J.; Lebaron, P.; Koblížek, M. Distribution of free-living and particle-attached aerobic anoxygenic phototrophic bacteria in marine environments. *Aquat. Microb. Ecol.* **2009**, *55*, 31–38. [[CrossRef](#)]
85. Hojerová, E.; Mašín, M.; Brunet, C.; Ferrera, I.; Gasol, J.M.; Koblížek, M. Distribution and growth of aerobic anoxygenic phototrophs in the Mediterranean Sea. *Environ. Microbiol.* **2011**, *13*, 2717–2725. [[CrossRef](#)] [[PubMed](#)]

86. Lamy, D.; Jeanthon, C.; Cottrell, M.T.; Kirchman, D.L.; Wambeke, F.V.; Ras, J.; Dahan, O.; Pujo-Pay, M.; Oriol, L.; Bariat, L.; et al. Ecology of aerobic anoxygenic phototrophic bacteria along an oligotrophic gradient in the Mediterranean Sea. *Biogeosciences* **2011**, *8*, 973–985. [[CrossRef](#)]
87. Jiao, N.; Zhang, Y.; Zeng, Y.; Hong, N.; Liu, R.; Chen, F.; Wang, P. Distinct distribution pattern of abundance and diversity of aerobic anoxygenic phototrophic bacteria in the global ocean. *Environ. Microbiol.* **2007**, *9*, 3091–3099. [[CrossRef](#)]
88. Ritchie, A.E.; Johnson, Z.I. Abundance and genetic diversity of aerobic anoxygenic phototrophic bacteria of coastal regions of the Pacific Ocean. *Appl. Environ. Microbiol.* **2012**, *78*, 2858–2866. [[CrossRef](#)]
89. Ferrera, I.; Borrego, C.M.; Salazar, G.; Gasol, J.M. Marked seasonality of aerobic anoxygenic phototrophic bacteria in the coastal NW Mediterranean Sea as revealed by cell abundance, pigment concentration and pyrosequencing of *pufM* gene. *Environ. Microbiol.* **2014**, *16*, 2953–2965. [[CrossRef](#)]
90. Yutin, N.; Suzuki, M.T.; Teeling, H.; Weber, M.; Venter, J.C.; Rusch, D.B.; Bèjà, O. Assessing diversity and biogeography of aerobic anoxygenic phototrophic bacteria in surface waters of the Atlantic and Pacific Oceans using the Global Ocean Sampling expedition metagenomes. *Environ. Microbiol.* **2007**, *9*, 1464–1475. [[CrossRef](#)]
91. Ferrera, I.; Gasol, J.M.; Sebastián, M.; Hojerová, E.; Koblížek, M. Growth rates of aerobic anoxygenic phototrophic bacteria as compared to other bacterioplankton groups in coastal Mediterranean waters. *Appl. Environ. Microbiol.* **2011**, *77*, 7451–7458. [[CrossRef](#)]
92. Ferrera, I.; Sarmiento, H.; Priscu, J.C.; Chiuchiolo, A.; González, J.M.; Grossart, H.P. Diversity and distribution of freshwater aerobic anoxygenic phototrophic bacteria across a wide latitudinal gradient. *Front. Microbiol.* **2017**, *8*, 175. [[CrossRef](#)]
93. Kirchman, D.L.; Stegman, M.R.; Nikrad, M.P.; Cottrell, M.T. Abundance, size, and activity of aerobic anoxygenic phototrophic bacteria in coastal waters of the West Antarctic Peninsula. *Aquat. Microb. Ecol.* **2014**, *73*, 41–49. [[CrossRef](#)]
94. Andersen, P.; Sorensen, H.M. Population dynamics and trophic coupling in pelagic microorganisms in eutrophic coastal waters. *Mar. Ecol. Prog. Ser.* **1986**, *33*, 99–109. [[CrossRef](#)]
95. Gonzalez, J.M.; Sherr, E.B.; Sherr, B.F. Size-selective grazing on bacteria by natural assemblages of estuarine flagellates and ciliates. *Appl. Environ. Microb.* **1990**, *56*, 583–589.
96. Šimek, K.; Chrzanowski, T.H. Direct and indirect evidence of size-selective grazing on pelagic bacteria by freshwater nanoflagellates. *Appl. Environ. Microbiol.* **1992**, *58*, 3715–3720.
97. Corinaldesi, C.; Crevatin, E.; Del Negro, P.; Marini, M.; Russo, A.; Fonda-Umani, S.; Danovaro, R. Large-scale spatial distribution of virioplankton in the Adriatic Sea: Testing the trophic state control hypothesis. *Appl. Environ. Microbiol.* **2003**, *69*, 2664–2673. [[CrossRef](#)]
98. Weinbauer, M.G.; Brettar, I.; Höfle, M.G. Lysogeny and virus-induced mortality of bacterioplankton in surface, deep, and anoxic marine waters. *Limnol. Oceanogr.* **2003**, *48*, 1457–1465. [[CrossRef](#)]
99. Magagnini, M.; Corinaldesi, C.; Monticelli, L.S.; De Domenico, E.; Danovaro, R. Viral abundance and distribution in mesopelagic and bathypelagic waters of the Mediterranean Sea. *Deep Sea Res. Part I Oceanogr. Res. Pap.* **2007**, *54*, 1209–1220. [[CrossRef](#)]
100. Magiopoulos, I.; Pitta, P. Viruses in a deep oligotrophic sea: Seasonal distribution of marine viruses in the epi-, meso- and bathypelagic waters of the Eastern Mediterranean Sea. *Deep Sea Res. Part I Oceanogr. Res. Pap.* **2012**, *66*, 1–10. [[CrossRef](#)]
101. Ordulj, M.; Krstulović, N.; Šantić, D.; Jozić, S.; Šolić, M. Distribution of marine viruses in the Central and South Adriatic Sea. *Mediterr. Mar. Sci.* **2015**, *16*, 65–72. [[CrossRef](#)]
102. Winter, C.; Köstner, N.; Kruspe, C.P.; Urban, D.; Muck, S.; Reinthaler, T.; Herndl, G.J. Mixing alters the lytic activity of viruses in the dark ocean. *Ecology* **2018**, *99*, 700–713. [[CrossRef](#)]
103. Baudoux, A.C.; Veldhuis, M.J.; Witte, H.J.; Brussaard, C.P. Viruses as mortality agents of picophytoplankton in the deep chlorophyll maximum layer during IRONAGES III. *Limnol. Oceanogr.* **2007**, *52*, 2519–2529. [[CrossRef](#)]

